

## Efficient Photoelectrochemical Reduction of Nitrite to Ammonium and Nitrogen Containing Gaseous Species Using Ti/TiO<sub>2</sub> Nanotube Electrodes

Fabiana A. Sayão, Luciana Nuñez and Maria V. B. Zanoni\*

Instituto de Química de Araraquara, Universidade Estadual Paulista “Júlio de Mesquita Filho” (UNESP), R. Prof. Francisco Degni, 55, P.O. Box 355, 14800-900 Araraquara-SP, Brazil

O presente trabalho descreve uma nova metodologia para remoção de nitrito de águas contaminadas usando o processo fotoeletrocatalítico. Um eletrodo de nanotubos de Ti/TiO<sub>2</sub> foi utilizado como fotocátodo sob irradiação UV e potencial aplicado -0,2 V vs. Ag/AgCl e levou a remoção de 100% do nitrito após 6 min de fotoeletrocatalise em solução de NaCl 7 mmol L<sup>-1</sup>, pH 7 e ausência de oxigênio dissolvido. A redução de nitrito sobre o eletrodo de Ti/TiO<sub>2</sub> ocorre no compartimento catódico da célula pelos elétrons fotogerados quando o eletrodo é irradiado com luz UV, gerando 7% de amônio e 93% de espécies gasosas de nitrogênio após 6 min de tratamento. Os resultados indicam que o método pode ser uma ferramenta eficiente para o tratamento de águas contaminadas com nitrito.

The present work describes a suitable method for removing nitrite contaminant from water by using a photoelectrocatalytical method. A Ti/TiO<sub>2</sub> nanotube electrode was used as a cathode under UV irradiation and applied potential of -0.2 V vs. Ag/AgCl and it led to 100% of nitrite removal after 6 min of photoelectrolysis conducted in NaCl 7 mmol L<sup>-1</sup>, pH 7 and in absence of dissolved oxygen. Nitrite reduction on Ti/TiO<sub>2</sub> photoelectrodes occurs in the cathodic compartment cell via electrons generated when the electrode is under UV irradiation leading to a generation of 7% of remaining ammonium and 93% nitrogen containing gaseous species after 6 min of treatment. The results indicate that the method could be an efficient tool for the treatment of nitrite in water containing nitrite.

**Keywords:** nitrite, photoelectrocatalysis, TiO<sub>2</sub> nanotubes, photocathode

### Introduction

Nitrite is an inorganic oxoanion of the nitrogen cycle and it can be formed by the reduction of the nitrate, which is the common nitrogen-containing compound naturally occurring in drinking water due to runoff from fertilizer use; leaching from septic tanks, sewage; and erosion of natural deposits.<sup>1</sup> It is frequently associated with the methemoglobinemia syndrome (blue baby syndrome) and cancers. Nitrites can react with secondary and tertiary amino compounds to form *N*-nitrous compounds diagnosed as potent carcinogens.<sup>2,3</sup> Although human exposure to nitrite also occurs by food intake,<sup>3</sup> making unnecessary its presence in water, since the World Health Organization (WHO) has established a maximum value of 3 mg L<sup>-1</sup> in water.<sup>2</sup>

Taking into account that biological treatment is the most useful process to remove nitrogen from water

and wastewater, incomplete nitrification culminates in accumulation of nitrite in the effluent and sometimes in activated sludge, wastewater reservoirs, rivers and live organisms.<sup>4,5</sup> The initial conversion of nitrate to nitrite, ammonium ions (NH<sub>4</sub><sup>+</sup>) and/or nitrogen-containing gaseous species is known from literature.<sup>6</sup> Thus, convenient methods able to remove nitrite from wastewater or coupled to biological treatment are very relevant to human and environment protection.

Literature reports several methods for nitrite removal.<sup>7-9</sup> The main methods applied to nitrite removal are based on physical, microbiological and chemical methods.<sup>7,10</sup> Physical methods include ionic membrane, reverse osmosis and electro dialysis. All these procedures are advantageous in a large scale and are efficient for minimizing nitrite concentration on wastewater treatment. But, they just promote phase separation, and produce waste with high concentrations.<sup>9-11</sup> Biological methods are based on microorganisms that use nitrite as a source of oxygen in

\*e-mail: boldrinv@yahoo.com.br

anaerobic conditions or, as sources of nitrogen as nutrient in aerobic conditions. The method is used as a first step of treatment and is able to treat a great volume of effluent, but promotes incomplete nitrification, has high cost and the need of subsequent treatment to reduce the generated sludge.<sup>10,12,13</sup> Chemical methods present the advantage to destroy or transform nitrite into a less toxic nitrogen form.<sup>7,8,10</sup> The most important are the catalytical processes, performed by metals such as Pd, Rh, Ru, Pt, Ni, Cu, Sn, Ag and Fe supported on non-stoichiometric oxides (such as TiO<sub>2</sub>, ZnO and Al<sub>2</sub>O<sub>3</sub>) associated with hydrogenation reactions or photocatalytic studies. These catalytical procedures show as an advantage, the capability of reducing nitrite and nitrate selectively into nitrogen containing gaseous species, whereas also requiring introduction of hydrogen gas or hole scavengers and high costs associated with the use of these noble metals.<sup>7-10,14-17</sup>

Among these methods, photoelectrocatalytic systems have been presented in the literature as a promising way to remove nitrate or nitrite from water.<sup>18-20</sup> Sun and Chou<sup>18</sup> have proposed a photoelectrocatalytic procedure for nitrite removal by oxidation on Ti/TiO<sub>2</sub> photoanode, resulting in nitrate as a product, which compared to nitrite is a less toxic nitrogen form for human health. More recently, Paschoal *et al.*<sup>19</sup> reported that bromate can be reduced into bromide at Ti/TiO<sub>2</sub> electrode under UV irradiation. Ti/TiO<sub>2</sub> acts as a photocathode when it is biased with negative potential in relation with the flat band potential. The system is preliminarily tested for nitrate reduction but there is no mention of nitrite reduction or generation.

The present paper investigates the conversion of nitrite by means of a photoelectrochemical process based on a Ti/TiO<sub>2</sub> nanotube electrode. The effect of bias potential and UV irradiation on efficiency of the photoelectrocatalytic reduction of nitrite was investigated by testing nitrate and ammonium formation. The goal was to propose a simple and rapid alternative method for treating water containing nitrite with high conversion to nitrogen-containing gaseous species.

## Experimental

### Preparation of TiO<sub>2</sub> nanotube electrode

Ti/TiO<sub>2</sub> nanotube electrode was prepared by self-organized TiO<sub>2</sub> nanotubes which were made by anodization of a titanium plate. Ti plate with an area of 25 cm<sup>2</sup> was cut and polished manually with sandpaper of different granulations, which were previously washed with detergent and ultrasonic bath with isopropyl alcohol, then acetone and finally after milli-Q water; all baths were 15 min long. After this procedure, the Ti plate was dried with compressed air.

Anodization was performed on an electrochemical cell by using a platinum electrode as a cathode. Cell was connected to the potentiostat (AUTOLAB, PGSTAT model 302), applying 30.5 V ( $v = 2V \text{ per min}$ ) for 50 hours, the supporting electrolyte of 0.15 mol L<sup>-1</sup> NH<sub>4</sub>F in 10% glycerol (Synth). After the anodization, the electrode was rinsed with milli-Q water, and dried with N<sub>2</sub> and finally was annealed at 450 °C for 30 minutes.

### Study of nitrite removal

For the purpose of evaluating the nitrite reduction efficiency by photoelectrocatalysis, the prepared Ti/TiO<sub>2</sub> nanotube photoelectrode was placed on a two-compartment glass reactor. The Pt gauze electrode was placed in the anodic compartment. At cathode compartment, the photoelectrode was placed as a work electrode, which was irradiated by an Hg (80 W) UV lamp vertically inserted in a central quartz glass bulb. An Ag/AgCl (KCl 3 mol L<sup>-1</sup>) electrode used as reference was placed close to the working electrode. The anode and cathode compartments were connected through a bridge tube containing a Vycor frit tip. The solution used in the reaction medium was of a concentration of 5 mg L<sup>-1</sup> nitrite in solution of 7 mmol L<sup>-1</sup> sodium chloride (Sigma-Aldrich), used as a supporting electrolyte.

In order to show the influence of dissolved oxygen in the solution, before the experiment, nitrogen gas was bubbled to remove the dissolved oxygen and, in another moment, to increase the concentration of dissolved oxygen, compressed air was bubbled as well.

In order to optimize the experimental conditions, studies on the influence of the applied potential were made from -0.6 to -0.2 V *vs.* Ag/AgCl, and the contribution of photocatalysis and photolysis on photoelectrocatalytic nitrite removal was evaluated.

### Instrumental

Photoelectrocatalysis experiments were performed using a Potentiostat/Galvanostat AUTOLAB (PGSTAT 302) for applying potential.

### Detection and monitoring of nitrate, nitrite and ammonium

Presence of nitrate and nitrite was analyzed by Thermo Scientific Dionex 1100 ion chromatography system, equipped with an anion analytical column ionPac® AS23 and a pre column ionPac® AG23, a mobile phase of Na<sub>2</sub>CO<sub>3</sub> 4.5 × 10<sup>-3</sup> mol L<sup>-1</sup>/NaHCO<sub>3</sub> 0.8 × 10<sup>-3</sup> mol L<sup>-1</sup>. Calibration curves were constructed for nitrate and nitrite concentrations from 0.2 to 30 mg L<sup>-1</sup> in triplicate, and a linear relationship was verified from the plot peak area *vs.*

concentration in  $\text{mg L}^{-1}$ , which followed the equation: Area =  $0.3188 + 1.1970 [\text{NO}_2^-]$ ,  $n = 7$ ,  $r = 0.998$  for nitrite and Area =  $-0.3953 + 1.1768 [\text{NO}_3^-]$ ,  $n = 7$  and  $r = 0.999$  for nitrate.

The ammonium generated was analyzed by ammonium detection test (Kit Ammonium-Test 1.14752.0001 Spectroquant®). The specific reactions were conducted on test tube and the product was analyzed by absorption at 690 nm on a Hewlett Packard spectrophotometer (HP-8453X). The calibration curve was constructed on a range of concentration of 0.002 to 2.0  $\text{mg L}^{-1}$  of ammonium, and a linear relationship was verified following the equation Area =  $0.0434 + 0.5529 [\text{NH}_4^+]$ ,  $n = 8$ ,  $r = 0.998$ .

The products generated from the photoelectrocatalytic reduction of nitrite are expressed as % of generation, which were calculated by the following equation:<sup>7-9</sup>

$$\% \text{ of product generation} = \left( \frac{\text{mol product formed}}{\text{mol NO}_2^- \text{ consumed}} \right) \times 100 \quad (1)$$

The % of generation of nitrogen-containing gaseous species (i.e.,  $\text{N}_2$ , NO and  $\text{NO}_2$ ) was calculated considering that all of the amount of nitrite which was consumed and was not detected as other products were converted to nitrogen-containing gaseous species.

## Results and Discussion

### Characteristics of the photocathode

Figure 1a illustrates the field emission scanning electron microscopy (FE-SEM) of Ti/TiO<sub>2</sub> photoelectrode. Arrays of TiO<sub>2</sub> nanotubes homogeneously distributed over the metallic Ti plate can be seen with a mean diameter of 100 nm and an average wall thickness of 10 nm. Figure 1b exhibits the X-ray diffractometry with diffraction peaks at  $2\theta = 35.2^\circ$  which is indexed as (101) crystal face of rutile, and, diffraction peaks at  $2\theta = 25.5, 37.3, 38.1, 48.2, 54.2$  and  $55.2^\circ$  which can be indexed as (101), (103) (004) (200) (105) and (211) faces of crystals of anatase, respectively.<sup>21</sup>

Curves of photocurrent vs. potential (Figure 2) were obtained for Ti/TiO<sub>2</sub> nanotube electrode in NaCl 7 mmol L<sup>-1</sup> in the absence of UV irradiation in solution containing dissolved oxygen (Figure 2A, curve a) and in the presence of light (Figure 2A, curve b). In atmosphere of nitrogen the photocurrent is negligible at dark (data not shown). The linear scan voltammograms obtained for oxygen reduction on Ti/TiO<sub>2</sub> electrode in the dark presented two electron transfer steps:  $\text{O}_{2\text{ads}} + 2e^- \rightarrow \text{H}_2\text{O}_2$  and  $\text{H}_2\text{O}_2 + 2e^- \rightarrow \text{H}_2\text{O}$ .<sup>22</sup> One is the production of water through a four-electron pathway around 0 V, and the other is the

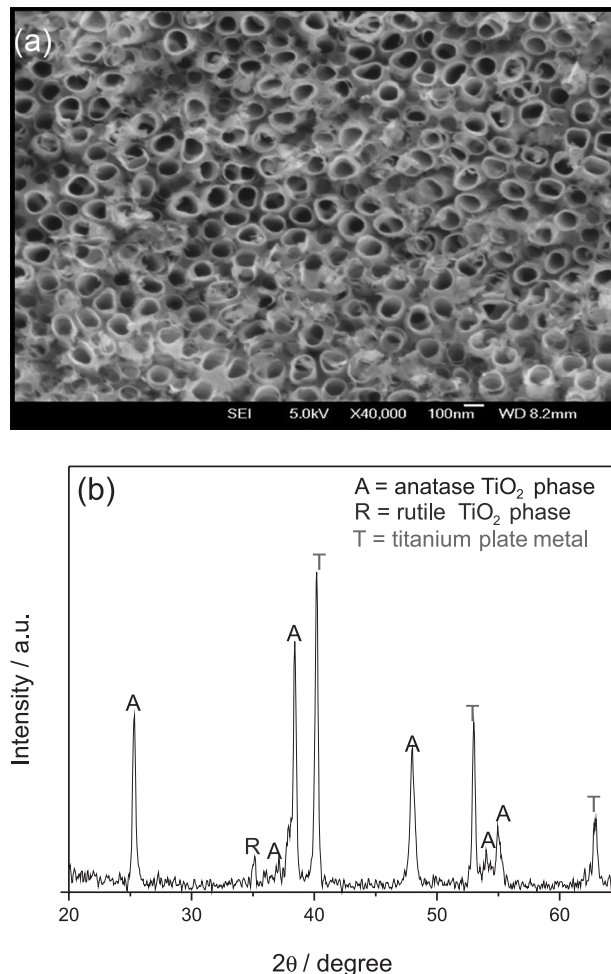


**Figure 1.** (a) Image of scanning electron microscopy obtained for Ti/TiO<sub>2</sub> nanotubes prepared through anodization of a Ti plate in 0.25%  $\text{NH}_4\text{F}$  in glycerol/10%  $\text{H}_2\text{O}$  (m/m) supporting electrolyte by applying 30 V for 50 hours after annealing at  $T = 450^\circ\text{C}$ . (b) X-ray diffraction pattern after annealing at  $450^\circ\text{C}$ . Ti: Titanium; A: Anatase.

production of hydrogen peroxide at  $-0.50$  V, through a two-electron pathway. Nevertheless, under UV irradiation, the cathodic wave is shifted to a more negative potential ( $-1.2$  V) (curve b) indicating that the system could be promoting the reduction of  $\text{O}_2$  to  $\text{O}_2^{\cdot-}$ , as in a conventional photocatalytic process.<sup>19,23,24</sup>

Under UV irradiation, the semiconductor acts as a catalyst activated by light of wavelength which can promote electrons from the valence band ( $b_v$ ) to the conduction band ( $b_c$ ). Thus, the electrons can act by reducing the oxygen adsorbed on the surface of the semiconductor at a more negative potential than the flat band potential of the semiconductor, generating the superoxide. On the other hand, at positive conditions, the holes are generated and act in oxidation reactions of water generating hydroxyl radicals with high oxidation power.<sup>25</sup> Therefore, a wave is observed at a potential more positive than 0.2 V, as shown on Figure 2A, curve b.

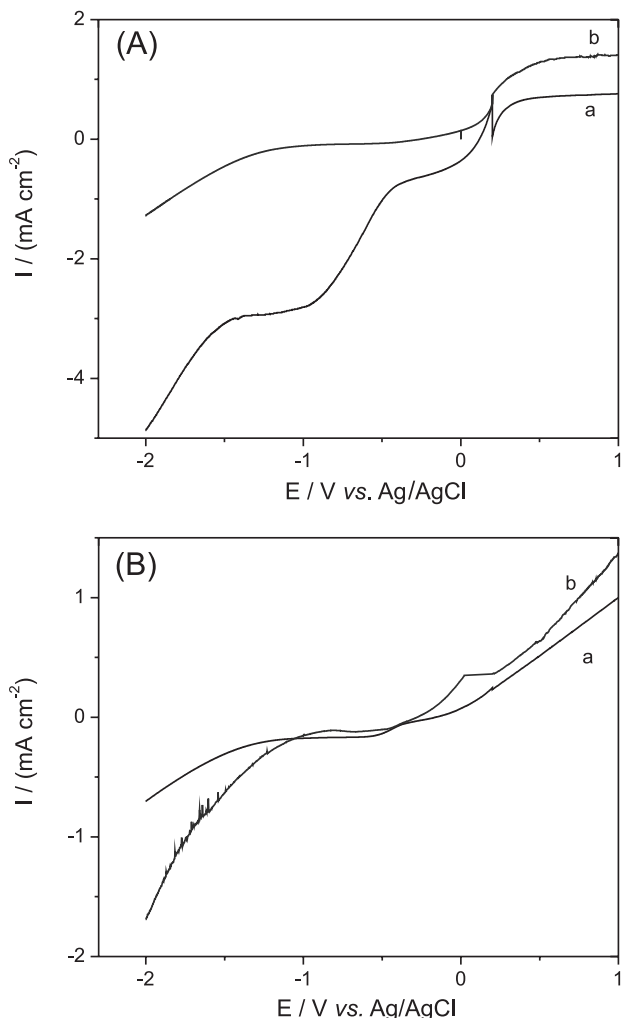


**Figure 2.** (A) Curves of density of photocurrent vs. potential obtained for Ti/TiO<sub>2</sub> nanotubes in 7 mmol L<sup>-1</sup> NaCl saturated with oxygen in the dark (a) and under UV irradiation (b). (B) Curves recorded under experimental condition of absence of dissolved oxygen containing 5 mg L<sup>-1</sup> of nitrite in 7 mmol L<sup>-1</sup> of NaCl in the dark (a) and under UV irradiation (b).

Although the photocurrent onset potential ( $E_{on}$ ) is often designated as the flat band potential ( $E_{fb}$ ), there are large uncertainties in these measurements, so the flat band potential for all electrodes was estimated using the Butler equation:<sup>26</sup>  $I_{ph}^2 = (2q \epsilon \epsilon_0 I_0^2 \alpha^2 / N_d) (E - E_{fb})$ ; where  $I_{ph}$  = photocurrent density,  $q$  = electron charge,  $\epsilon$  = dielectric constant,  $\epsilon_0$  = permittivity of free space,  $I_0$  = photon flux,  $\alpha$  = absorption coefficient for solids,  $N_d$  = effective density of states at the conduction band edge,  $E$  = potential,  $E_{fb}$  = flat band potential. Thus, from the linear graph of  $I_{ph}^2$  vs. the applied potential (data not show here) an  $E_{fb} = -0.199$  V vs. Ag/AgCl was obtained for Ti/TiO<sub>2</sub> nanotubes in NaCl saturated with oxygen.

In order to observe the effect of nitrite on the photoactivity of the electrodes, curves of photocurrent vs. potential were recorded by linear scan voltammetry (10 mV s<sup>-1</sup>) for the reduction of 5 mg L<sup>-1</sup> of nitrite in

7 mmol L<sup>-1</sup> NaCl in the absence of oxygen under UV irradiation (Figure 2B, curve b) and dark conditions (Figure 2B, curve a). According to Figure 2B (curve a), the presence of nitrite elicits a small wave around +0.20 V, indicating that nitrite is acting as an efficient electron scavenger, i.e., nitrite captures the photoelectrons generated on the photoelectrode more efficiently. The photocurrent corresponds to the balance between light absorption by the Ti/TiO<sub>2</sub> layer and the production of electron-hole pairs:  $Ti/TiO_2 + h\nu \rightarrow h_{bv}^+ + e_{bc}^-$ . Combined with UV irradiation, the applied potential bends the bands in the region of the electrode/electrolyte interface where the electrons and holes are effectively separated. The voltammetric curve attests that the potential shifts 150 mV toward less negative values compared with the solution in the dark (curve b). Therefore, we carried out further experiments at an applied potential of -0.2 V vs. Ag/AgCl, which is enough to promote competitive photoelectroreduction of nitrite on the Ti/TiO<sub>2</sub> electrode irradiated with UV light. The results indicate that, under applied potentials below the flat band potential, there is a bending band which drives the photogenerated electrons from the bulk to the oxide surface, and makes them available to promote reduction reaction with species adsorbed preferentially on the semiconductor surface. At the counter electrode compartment water oxidation occurs. In order to investigate the photoelectrocatalytic nitrite removal, new photoelectrolyses were carried out using bias voltage equal to or more negative than the calculated value of the flat band potential of the electrode under UV irradiation.

#### Photoelectrocatalytic oxidation of nitrite

Figure 3 exhibits the photoelectrocatalytic reduction of 5 mg L<sup>-1</sup> nitrite in 7 mmol L<sup>-1</sup> of NaCl at Ti/TiO<sub>2</sub> electrode under bias potential of -0.2 V vs. Ag/AgCl and an irradiation at UV region. Under these conditions, it is shown the reduction of up to 86% nitrite after 60 min of treatment at the cathodic compartment. On the other hand, nitrite is not reduced at the anodic compartment. It is also observed that there is no significant nitrite reduction in the cathodic compartment when direct electrolysis is performed at -0.20 V without UV irradiation, regardless of the applied potential (data not shown). The dependence of the initial NO<sub>2</sub><sup>-</sup> degradation rate was evaluated from the slope of the curve obtained for the NO<sub>2</sub><sup>-</sup> consumption (% mg L<sup>-1</sup>) as a function of time (min). The reduction decreased linearly, following the equation  $\ln C / C_0 = -k t$ , where  $C$  = NO<sub>2</sub><sup>-</sup> concentration at time  $t$ ,  $C_0$  = NO<sub>2</sub><sup>-</sup> concentration at time = 0, and  $k$  = rate constant. This suggests that the initial rate for

$\text{NO}_2^-$  reduction follows a pseudo first-order process, with a constant rate of  $0.03 \text{ min}^{-1}$ .

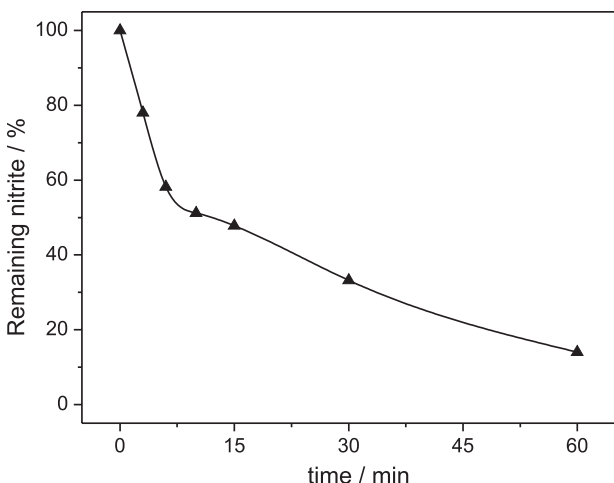
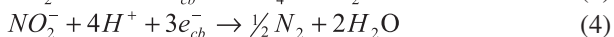
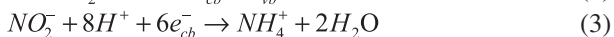


**Figure 3.** Photoelectrocatalytic removal of  $5 \text{ mg L}^{-1}$  of nitrite in  $7 \text{ mmol L}^{-1}$  of NaCl using Ti/TiO<sub>2</sub> electrode under applied potential of  $-0.2 \text{ V vs. Ag/AgCl}$  and UV irradiation.

So, in agreement with the literature,<sup>19</sup> nitrite reduction on Ti/TiO<sub>2</sub> photoelectrodes could happen in the cathodic compartment cell via electrons generated under UV irradiation and driven to the electrode surface. On the other hand, there is no nitrite reduction in the counter electrode compartment cell, indicating that only water oxidation takes place in the counter electrode, according to the following equations:<sup>27-30</sup>

Photocathode:



Anode:



In agreement with the above equations nitrite photoreduction can lead to generation of ammonium ions and nitrogen as a main subproduct and/or other nitrogen-containing gases, which was not quantified since the literature reports that they are not representative in the process.<sup>8</sup>

Parameters affecting the photoelectrocatalytic reduction of nitrite

It is well known that dissolved oxygen in solution can act as a photogenerated electron trapper in the photoelectrocatalytic process.<sup>31</sup> Therefore, the effect of dissolved oxygen on nitrite reduction was investigated

by monitoring the reduction of  $5 \text{ mg L}^{-1}$  of nitrite by photoelectrocatalysis on Ti/TiO<sub>2</sub> electrode under an applied potential of  $-0.2 \text{ V vs. Ag/AgCl}$  and UV irradiation. These experiments were performed in (i) solution saturated with oxygen using compressed air; (ii) original solution with air dissolved naturally; and (iii) deaerated with nitrogen gas to remove dissolved O<sub>2</sub> in the original solution. The nitrite removal during 60 min of treatment is shown in Figure 4. It is evident that under dissolved O<sub>2</sub> or air (curve a) nitrite removal efficiency is dramatically reduced in relation to the original solution (curve b). Further studies were carried out by using oxygen removal by bubbling nitrogen during the experiments. Under deaerated solution (curve c) it was possible to obtain 100% of nitrite reduction after 6 min of photoelectrocatalysis, revealing that the dissolved oxygen acts negatively on the reduction of nitrite by photoelectrocatalytic procedure on TiO<sub>2</sub> surface.

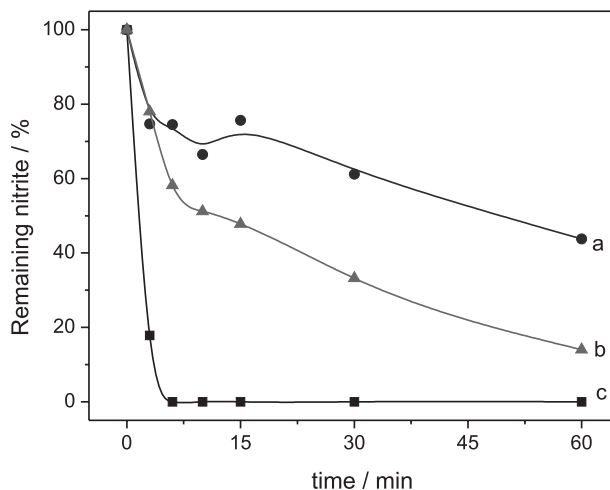


**Figure 4.** Influence of dissolved oxygen on the photoelectrocatalytic reduction of  $5 \text{ mg L}^{-1}$  of nitrite in  $7 \text{ mmol L}^{-1}$  of NaCl at applied potential of  $-0.2 \text{ V vs. Ag/AgCl}$  with UV irradiation. (a) saturated with dissolved oxygen; (b) dissolved air; and (c) saturated with nitrogen gas.

In order to understand the effect of applied potential on the reduction of nitrite at Ti/TiO<sub>2</sub> nanotube electrodes, further experiments were carried out to determine the efficiency of photoelectrocatalytic oxidation (Ti/TiO<sub>2</sub> under UV irradiation and  $E = -0.20 \text{ V vs. Ag/AgCl}$ ) in comparison with photolysis (UV irradiation) and photocatalysis (Ti/TiO<sub>2</sub> catalyst under UV irradiation). Therefore, the reduction of  $5 \text{ mg L}^{-1}$  of nitrite was monitored in  $7 \text{ mmol L}^{-1}$  of NaCl. The response was analysed by the relative decrease of the nitrite concentration and the results are shown in Figure 5. On the photolytic experiment, there was a 60% of removal of nitrite (Figure 5a) after 60 min of treatment. The photolysis of nitrite was expected because under UV light nitrite is converted into nitrate and, also nitrate is converted into nitrite, and since the equilibrium reactions are dependent

on temperature and pH,<sup>32</sup> the variations of these parameters during experiment should be responsible for the increase on nitrite amount observed on curve a after 30 minutes. The removal of nitrite by photocatalytic process (Figure 5b) reached 67% after 60 min of treatment, but after some time the photocatalytic process was proven to be less efficient compared to a simple photolytic process (Figure 5a). It probably happens because under photocatalytic conditions nitrite is reduced by photogenerated electron, but nitrite can also be oxidized by photogenerated hole converting part of it into a nitrate form.<sup>33</sup> These concomitant reactions are probably responsible for the lower efficiency of photocatalytic and photolytic processes when compared to a photoelectrocatalytic process that promotes charge separation.

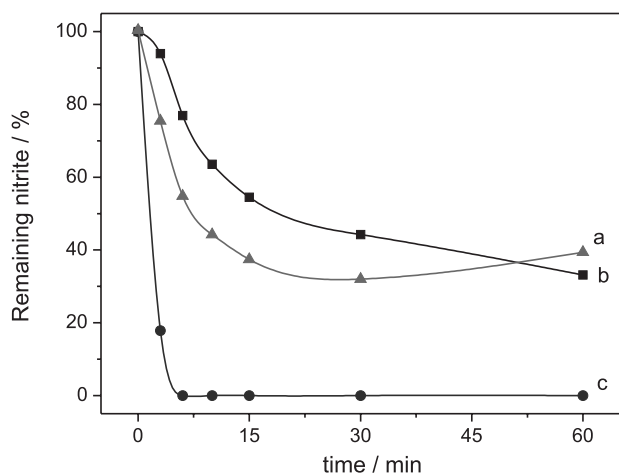


**Figure 5.** Removal of nitrite in the absence of dissolved oxygen during (a) photolysis (UV irradiation); (b) photocatalysis (UV irradiation + catalyst); and (c) photoelectrocatalysis (UV irradiation + catalyst +  $E = -0.2$  V vs. Ag/AgCl) in 7 mmol L<sup>-1</sup> of NaCl.

Using the photoelectrocatalytic treatment (Figure 5c) and the absence of dissolved oxygen, complete nitrite removal occurred after 6 min of treatment. The increase of removal of nitrite on photoelectrocatalytic process can be explained by minimizing the recombination process by applied potential. For all processes involving nitrite reduction, the process follows a pseudo first order decay and, the rate constants ( $k$ ) correspond to 0.01, 0.04 and 0.57 min<sup>-1</sup> for the photolytic, photocatalytic and photoelectrocatalytic experiments, respectively. The experiment shows that the nitrite photoelectrocatalytic reduction occurs at a rate 57 times greater than the simple photocatalysis of nitrite, suggesting that the combination of potential and UV irradiation could be an efficient way to remove nitrite in aqueous solution.

The effect of bias potential in the nitrite reduction was investigated comparing the performance of

photoelectrocatalytic reduction operating at Ti/TiO<sub>2</sub> under applied potential of  $-0.6$ ,  $-0.4$  and  $-0.2$  V and UV irradiation in absence of dissolved oxygen. Figure 6 illustrates that the total reduction of nitrite is reached after 6 min that the photoelectrolysis is conducted at  $-0.4$  and  $-0.2$  V (curves b and c, respectively). On the other hand, 100% of nitrite reduction is reached after photoelectrolysis is conducted for 15 min under bias voltage of  $-0.6$  V (curve a). The rate constants ( $k$ ) of the nitrite reduction were calculated, corresponding to 0.57, 0.26 and 0.14 min<sup>-1</sup> for the potential of  $-0.2$ ,  $-0.4$  and  $-0.6$  V vs. Ag/AgCl, respectively, therefore indicating that a less negative potential ( $-0.2$  V) improves the efficiency of the method. These results agree with the results previously obtained by using electrodes of Ti/TiO<sub>2</sub> photoelectrocatalytic reduction of oxoanion bromate.<sup>19</sup>

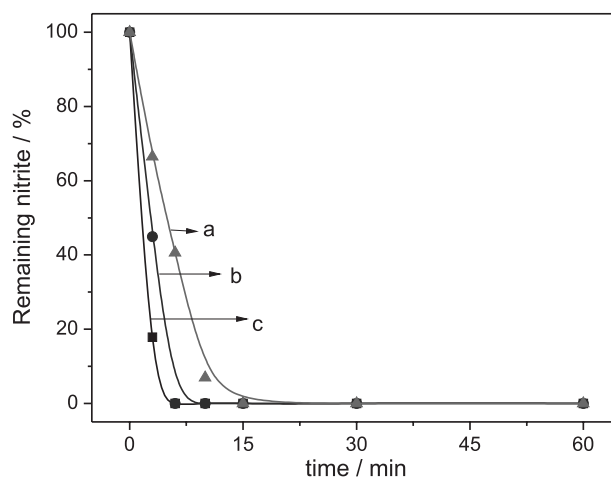


**Figure 6.** Effect of applied potential in the photoelectrocatalytic reduction of 5 mg L<sup>-1</sup> of nitrite at Ti/TiO<sub>2</sub> electrode under potential: (a)  $-0.6$  V; (b)  $-0.4$  V; and (c)  $-0.2$  V vs. Ag/AgCl and UV radiation in 7 mmol L<sup>-1</sup> of NaCl and absence of dissolved oxygen.

Taking into consideration that nitrite reduction can usually generate NH<sub>4</sub><sup>+</sup> and/or nitrogen-containing gaseous species,<sup>34,35</sup> the amount of produced NH<sub>4</sub><sup>+</sup> was determined during the photoelectrocatalysis conducted for nitrite removal using the best previously defined experimental condition. Figure 7 illustrates the photoelectrocatalytic reduction of 5 mg L<sup>-1</sup> of nitrite in 7 mmol L<sup>-1</sup> of NaCl at Ti/TiO<sub>2</sub> nanotube electrode under  $-0.2$  V and 80 W UV irradiation without dissolved oxygen (curve a) and the concomitant generation of nitrate (curve b); ammonium (curve c) and nitrogen-containing gaseous species (curve d).

The results indicate that 100% of nitrite removal is obtained in the first 6 min of treatment. Concomitantly, there is no formation of nitrate, but there is successive increase of ammonium generation up to 44% after 60 min of treatment. In addition, the electrolysis promoted up to 56% conversion

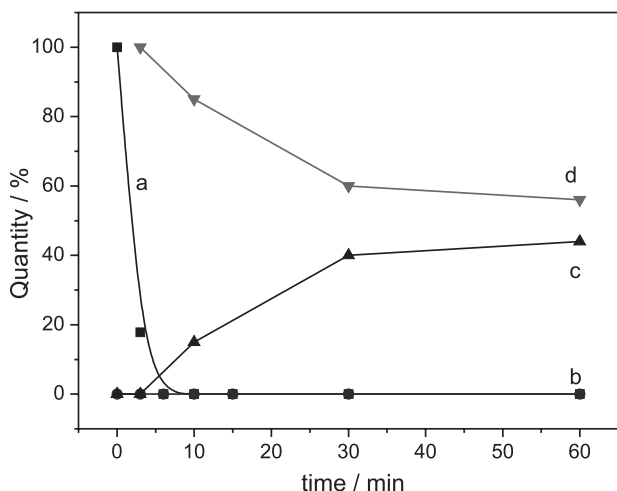


**Figure 7.** Photoelectrocatalytical reduction of 5 mg L<sup>-1</sup> of nitrite in 7 mmol L<sup>-1</sup> of NaCl, at Ti/TiO<sub>2</sub> nanotube electrode under -0.2V vs. Ag/AgCl and UV irradiation without dissolved O<sub>2</sub>. (a) remaining nitrite; (b) nitrate generation; (c) ammonium generation; and (d) nitrogen-containing gaseous species.

to gaseous species. These results are very interesting since there is no formation of nitrate and if reaction is stopped at 6 minutes there is a good selectivity (93%) for nitrogen-containing gaseous species and only 7% for ammonium. As the maximum limit recommended for nitrite in drinking water is 3 mg L<sup>-1</sup> (WHO), the proposed method could be successfully applied to remove nitrite from drinking water.

## Conclusions

Our finding indicates that photoelectrocatalysis can be used as a good alternative to remove nitrite from water by using its reduction at Ti/TiO<sub>2</sub> nanotube electrode prepared by electrochemical anodization. The best experimental condition for its removal was found under the applied potential of -0.20 V, UV irradiation in the absence of dissolved oxygen. The results indicate that 100% of nitrite can be reached after 60 min of treatment in 7 mmol L<sup>-1</sup> of NaCl as a supporting electrolyte in the absence of dissolved oxygen. The resulting electrode is stable and reach 7 % of the remaining ammonium and 93 % of nitrogen containing gaseous species at 6 minutes of treatment.

## Acknowledgments

The authors thank FAPESP (2008/10449-7), CNPq and CAPES for their financial support.

## References

- Canter, L. W.; *Nitrates in Groundwater*, CRC Press: Boca Raton, USA, 1997.

- World Health Organization (WHO); *Guidelines for Drinking-Water Quality*, 4<sup>th</sup> ed.; WHO Press: Geneva, 2011, p. 564.
- Lijinsky, W.; *Ambio* **1976**, 5, 67.
- Alleman, J. E.; *Water Sci. Technol.* **1984**, 17, 409.
- Randall, C. W.; Buth, D.; *J. Water Pollut. Control Fed.* **1984**, 56, 1039.
- Ranjit, K. T.; Varadarajan, T. K.; Viswanathan, B.; *J. Photochem. Photobiol., A* **1995**, 89, 67.
- Barrabés, N.; Sá, J.; *Appl. Catal., B* **2011**, 104, 1.
- Constantinou, C. L.; Costa, C. N.; Efstathiou, A. M.; *Catal. Today* **2010**, 151, 190.
- Kapoor, A.; Viraraghavan, T.; *J. Environ. Eng.* **1997**, 123, 371.
- Archana; Sharma, S. K.; Sobti, R. C.; *E-J. Chem.* **2012**, 9, 1667.
- Mateju, V.; Cizinska, S.; Krejci, J.; Janoch, T.; *Enzyme Microb. Technol.* **1992**, 14, 170.
- Adav, S. S.; Lee, D.; Lai, J. Y.; *Appl. Microbiol. Biotechnol.* **2010**, 85, 773.
- Kamat, S.; Sabatini, D. A.; Canter, L. W.; *Environ. Pollut.* **1991**, 65, 25.
- Zhang, Y.; Lu, J.; Wu, L.; Chang, A.; Frankenberger Jr., W. T.; *Sci. Total Environ.* **2007**, 382, 383.
- Ranjit, K. T.; Varadarajan, T. K.; Viswanathan, B.; *J. Photochem. Photobiol., A* **1996**, 96, 181.
- Ranjit, K. T.; Viswanathan, B.; *J. Photochem. Photobiol., A* **1997**, 108, 73.
- Gekko, H.; Hashimoto, K.; Kominami, H.; *Phys. Chem. Chem. Phys.* **2012**, 14, 7965.
- Sun, C. C.; Chou, T. C.; *J. Mol. Catal. A: Chem.* **2000**, 151, 133.
- Paschoal, F. M. M.; Pepping, G.; Zanoni, M. V. B.; Anderson, M. A.; *Environ. Sci. Technol.* **2009**, 43, 7496.
- Mor, G. K.; Varghese, O. K.; Paulose, M.; Shankar, K.; Grimes, C. A.; *Sol. Energy Mater. Sol. Cells* **2006**, 90, 2011.
- de Lagemaat, J. V.; Plakman, M.; Vanmaekelbergh, D.; Kelly, J. J.; *Appl. Phys. Lett.* **1996**, 69, 2246.
- Wang, B.; *J. Power Sources* **2005**, 152, 1.
- Paschoal, F. M. M.; Nuñez, L.; Lanza, M. R. V.; Zanoni, M. V. B.; *J. Adv. Oxid. Technol.* **2013**, 16, 63.
- Blesa, M. A.; *Eliminación de Contaminantes por Fotocatálisis Heterogénea*; Cooperacion Iberoamericana: Buenos Aires, 2001, p. 316.
- Fujishima, A.; Rao, T. R.; Tryk, D. A.; *J. Photochem. Photobiol., C* **2000**, 1, 1.
- Butler, M. A.; *J. Appl. Phys.* **1977**, 48, 1914.
- Kato, H.; Kudo, A.; *Phys. Chem. Chem. Phys.* **2002**, 4, 2833.
- Ranjit, K. T.; Varadarajan, T. K.; Viswanathan, B.; *J. Photochem. Photobiol., A* **1995**, 89, 67.
- Sá, J.; Agüerra, A.; Gross, S.; Anderson, J. A.; *Appl. Catal., B* **2009**, 85, 192.
- Ohtani, B.; Kakimoto, M.; Miyadzu, H.; Nishimoto, S.; Kagiya, T.; *J. Phys. Chem.* **1988**, 92, 5773.

31. Scharz, F. P.; Turro, N. J.; Bossmann, S. H.; Braun, A. M.; Wahab, A. A. A.; Diirr, H.; *J. Phys. Chem. B* **1997**, *101*, 7127.
32. Mack, J.; Bolton, J. R.; *J. Photochem. Photobiol., A* **1999**, *128*, 1.
33. Shifu, C.; Gengyu, C.; *Sol. Energy* **2002**, *73*, 15.
34. Pintar, A.; Batista, J.; Levec, J.; Kajiuchi, T.; *Appl. Catal., B* **1996**, *11*, 81.
35. Prusse, U.; Hähnlein, M.; Daum, J.; Vorlop, K.; *Catal. Today* **2000**, *55*, 79.

*Submitted: November 7, 2013*

*Published online: April 29, 2014*

**FAPESP has sponsored the publication of this article.**